BEILSTEIN JOURNAL OF ORGANIC CHEMISTRY

Additive-controlled chemoselective inter-/intramolecular hydroamination via electrochemical PCET process

Kazuhiro Okamoto, Naoki Shida* and Mahito Atobe*

Full Research Paper

Open Access

Address:
Graduate School of Engineering, Yokohama National University, 79-7 Tokiwadai, Hodogaya-ku, Yokohama, Kanagawa 240-8501, Japan

Email:
Naoki Shida* - shida-naoki-gz@ynu.ac.jp; Mahito Atobe* - atobe@ynu.ac.jp

* Corresponding author

Keywords:
amidyl radical; cyclic voltammetry; electrosynthesis; hydroamination; proton coupled electron transfer

Beilstein J. Org. Chem. **2024,** *20,* 264–271.
https://doi.org/10.3762/bjoc.20.27

Received: 04 December 2023
Accepted: 01 February 2024
Published: 12 February 2024

This article is part of the thematic issue "Synthetic electrochemistry".

Guest Editor: K. Lam

Abstract

Electrochemically generated amidyl radical species produced distinct inter- or intramolecular hydroamination reaction products via a proton-coupled electron transfer (PCET) mechanism. Cyclic voltammetry (CV) analysis indicated that the chemoselectivity was derived from the size of the hydrogen bond complex, which consisted of the carbamate substrate and phosphate base, and could be controlled using 1,1,1,3,3,3-hexafluoro-2-propanol (HFIP) as an additive. These results provide fundamental insights for the design of PCET-based redox reaction systems under electrochemical conditions.

Introduction

Proton-coupled electron transfer (PCET) enables the generation of various radical species under ambient conditions (Figure 1, top) [1]. In PCET processes, hydrogen bond formation between weak bases and acidic X–H bonds (X = N, O, C) is a key step, which is followed by concerted proton- and electron-transfer to give the corresponding radical species through oxidative X–H bond cleavage. One such species is the amidyl radical, which is broadly synthetically useful as a nitrogen source in hydroamination reactions and as a hydrogen atom transfer (HAT) reagent for remote C–H activation [2-8]. Recent advances in photoredox and electrochemical PCET reactions have significantly expanded the substrate scope of amidyl-radical-based molecular transformations because the harsh acidic and high-temperature conditions required in the classical Hofmann–Löffler–Freytag reaction can be avoided [9].

The initial aim of this study was the electrochemical generation of an amidyl radical as a HAT source for the synthesis of 1'-*C* functionalized nucleosides via the generation of an anomeric radical species from uridine derivative **1** (Figure 1, bottom) [10]. Although the HAT reaction failed, remarkable inter- and intramolecular chemoselectivities were observed in the hydro-

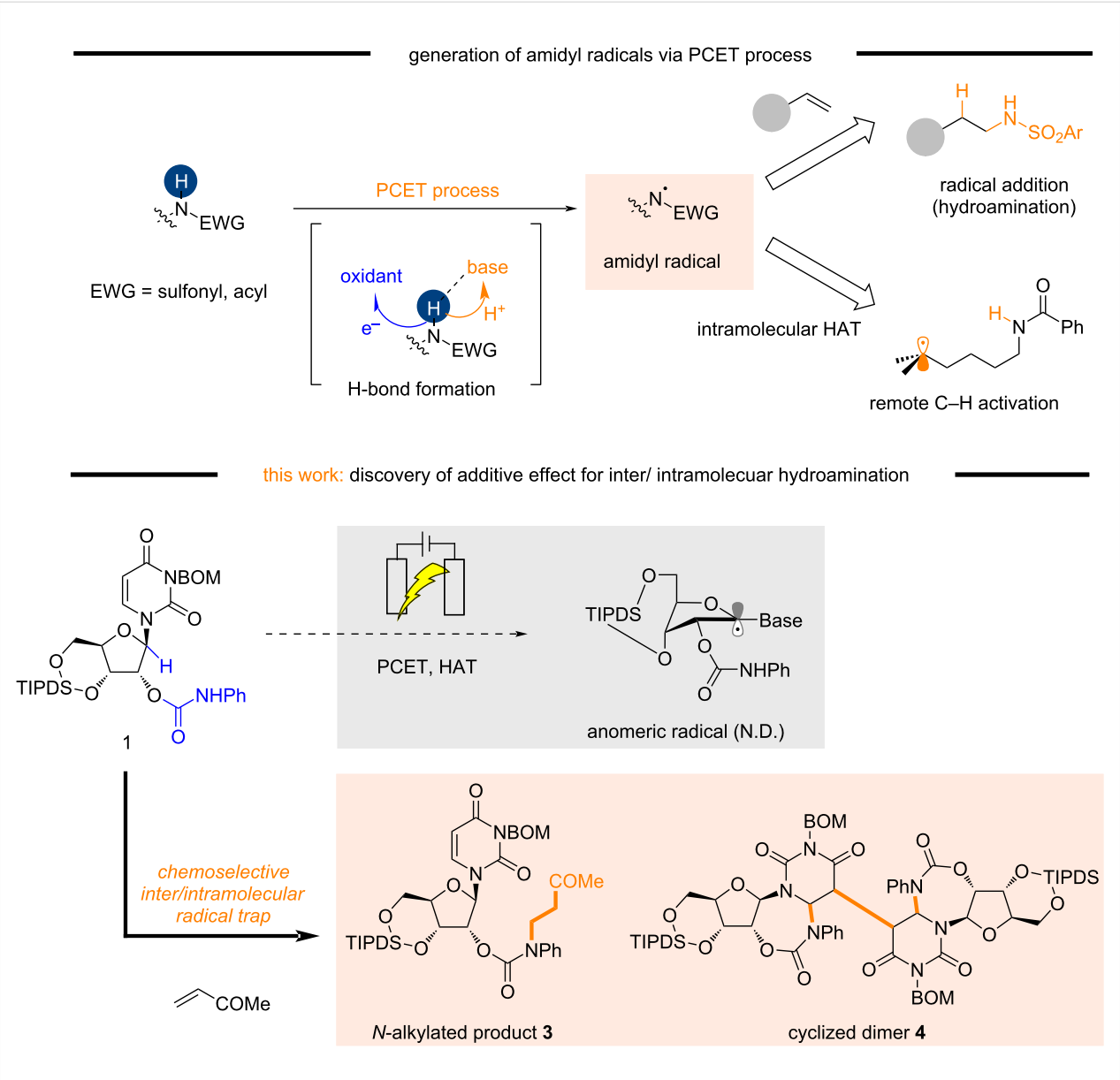

Figure 1: Application of amidyl radical species generated by PCET.

amination reaction. We investigated this phenomenon and found that complete inter-/intramolecular chemoselectivity could be achieved by modifying the reaction conditions, despite the presence of both inter- and intramolecular radical acceptor moieties. Therefore, we investigated the origin of this selectivity under electrochemical conditions.

Results and Discussion

Anodic oxidation of uridine derivative **1** was performed in a CH_2Cl_2/Bu_4NPF_6 (0.1 M) electrolyte system using a carbon felt (CF) anode and a Pt cathode in the presence of methyl vinyl ketone (MVK) as a radical acceptor (Table 1). Tetrabutylammonium dibutyl phosphate (phosphate base), which operates as a PCET initiator through hydrogen bond formation with the N–H bond of amide/carbamate [11], was used as an additive. As a result, *N*-alkylated product **3** was exclusively obtained, implying that the expected HAT at the 1'-*C* position to afford **2** (Table 1, entry 1) had not occurred. In contrast, the reaction efficiency was significantly decreased in the absence of the phosphate base (Table 1, entry 2), and electricity is necessary to proceed the reaction (Table 1, entry 3); thus, the phosphate base plays a crucial role in *N*-alkylation, while its basicity is insufficient to promote aza-Michael addition (pK_a of the conjugate acid of the phosphate base is 1.72 in H_2O) [12]. Furthermore, *N*-alkylation proceeded in a divided cell (anodic chamber); thus, the possibility of conjugate addition of a cathodically generated

Table 1: Electrochemical oxidation of **1** under varying conditions.

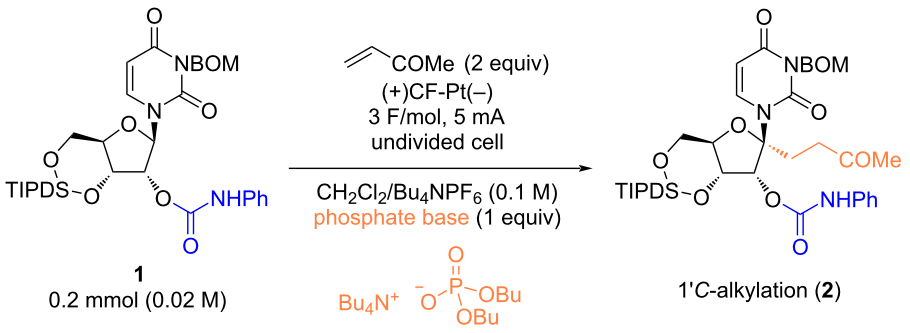

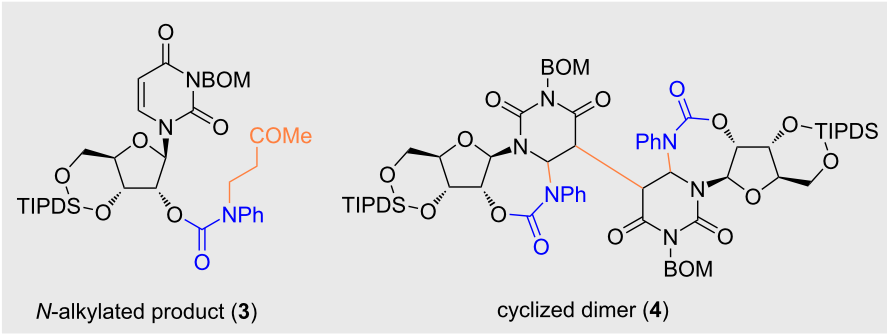

Entry	Deviation from standard conditions	Yield [%][a]	Recovered **1** [%][a]
1	none	57, 49[b] (**3**)	17
2	without phosphate base	13 (**3**)	76
3	without electricity	N.R.	92
4	divided cell (anodic chamber)	41 (**3**)	27
5	HFIP (2 equiv) as an additive	42, 27[b] (**4**)	32
6	AcOH (2 equiv) as an additive	10 (**3**)	51
7	MeCN instead of CH_2Cl_2	17 (**4**)	28

[a]Yield was determined based on ^{1}H NMR by using benzaldehyde as an internal standard, and recovery rate of **1** was determined by the integral of H-1' proton. [b]Isolated yield.

carbamate anion was ruled out, prompting us to consider that *N*-alkylation proceeded via a radical mechanism. On the other hand, the addition of 1,1,1,3,3,3-hexafluoro-2-propanol (HFIP) led to the predominant formation of cyclized dimer **4** without *N*-alkylation, whereas the use of AcOH provided *N*-alkylated product **3** (Table 1, entries 5 and 6). When acetonitrile (MeCN) was used as the solvent, cyclized dimer **4** was obtained (Table 1, entry 7).

Next, **1** was subjected to cyclic voltammetry (CV) measurements under varying conditions (Figure 2). An oxidation wave was observed at approximately +1.4 V (Figure 2A). The oxidation current of this wave decreased significantly in the presence of a phosphate base and the subsequent addition of HFIP enhanced this phenomenon (Figure 2B, grey line). In contrast, using AcOH instead of HFIP did not affect the oxidation current (Figure 2B, blue line). We considered that the inter- and intramolecular chemoselectivities were derived from the pK_a of the proton sources.

The pre-organization of the amide substrate and phosphate bases is an important process in PCET [13]. Recently, Gschwind et al. published a detailed NMR spectroscopic analysis of a PCET-mediated hydroamination reaction, which indicated that the pK_a of the proton source (PhSH or PhOH in the study) determines the size of the hydrogen bond complex. PhSH as the more acidic additive (pK_a = 6.62 in H_2O) provided better results in the PCET-induced intramolecular hydroamination reaction compared to the less acidic PhOH (pK_a = 9.95 in H_2O) because PhSH supplied free protons (H^+) and contributed to the

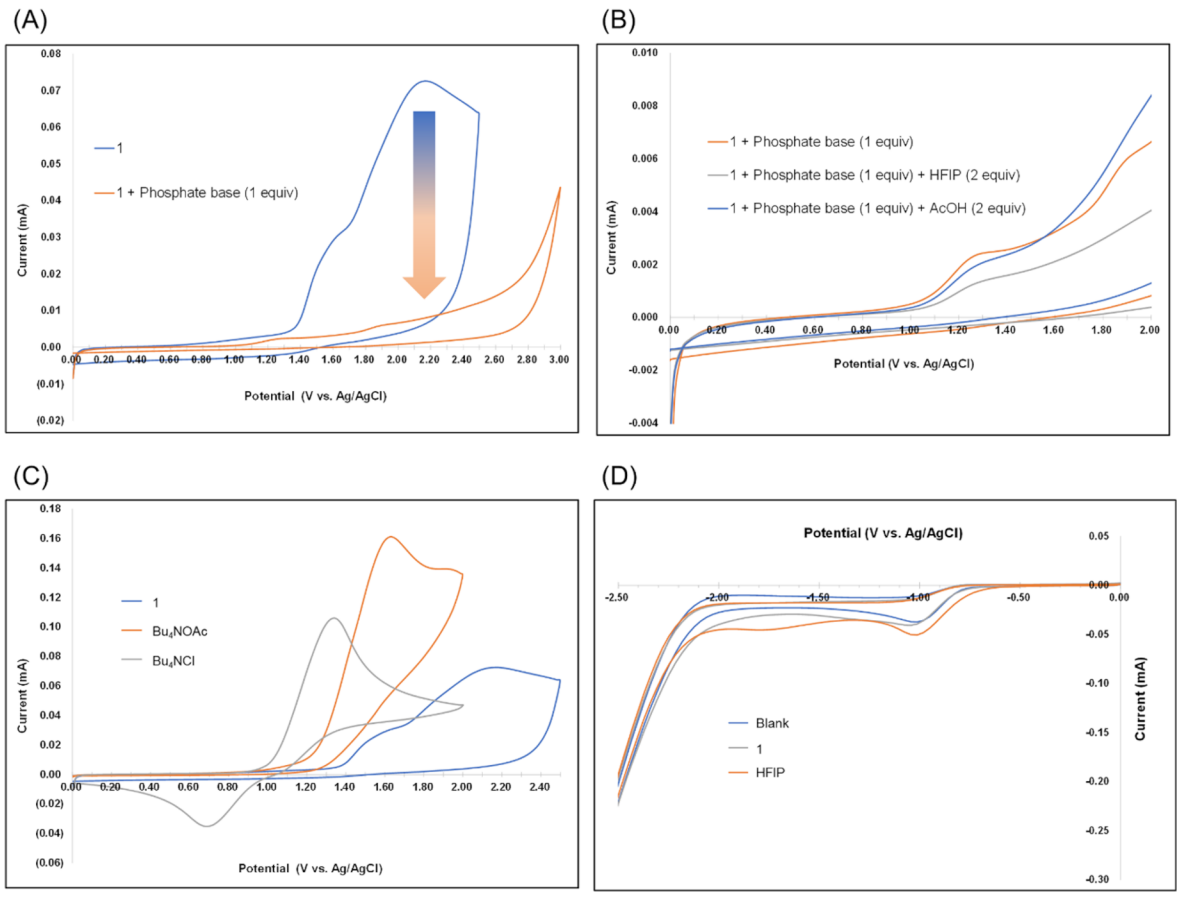

Figure 2: (A) Effect of phosphate base on the cyclic voltammogram of **1**. (B) Cyclic voltammograms of **1** in the presence of additives (AcOH or HFIP). (C) Comparison of oxidation potentials of **1** using Bu_4NOAc or Bu_4NCl. (D) Cyclic voltammograms for the cathodic side. All cyclic voltammograms were recorded in CH_2Cl_2/Bu_4NPF_6 (0.1 M). Sample concentration was 0.01 M. A glassy carbon anode (φ 3 mm) and Pt cathode (φ 3 mm) were used. Scan rate = 100 mV/s.

persistence of small aggregates composed of the amide and phosphate base [14]. On the other hand, owing to the insufficient dissociation constant between the proton and phenoxide in PhOH, the PhOH molecule is included in the hydrogen bond network along with the tetrabutylammonium cation (Bu_4N^+) to form a large aggregate. The hydrogen bonding between the amide and phosphate base in the small aggregates was stronger than in the large aggregates, which significantly enhanced amidyl radical generation through the PCET mechanism.

The above studies provided us with valuable insights into the intriguing electrochemical behavior of **1** (Figure 3). Hydrogen bond formation between **1** and the phosphate base yielded small aggregates, the interaction efficiency of which with the electrode surface was lower than that of **1** because the relatively large hydrodynamic radius of the aggregates decreased the number of electrode-accessible molecules. This increase in the hydrodynamic radius resulted in a decrease in the oxidation current. In the present study, HFIP (pK_a = 9.30 in H_2O) [15] is less acidic than AcOH (pK_a = 4.76 in H_2O) with a pK_a value similar to that of PhOH, which forms large aggregates under PCET conditions, as described above. Therefore, analogously, HFIP is expected to be included in the hydrogen-bonded complex. The resulting large aggregates further impeded access to the electrode surface, and a further decrease in the oxidation current was observed in the presence of HFIP (Figure 2B, grey line). In contrast, the more acidic AcOH supplied free protons, which enabled the persistence of small aggregates; thus, the current was not affected by the presence of AcOH (Figure 2B, blue line). However, in the presence of AcOH, the *N*-alkylation yield was low (Table 1, entry 6) owing to the competitive Kolbe oxidation of the cathodically generated acetate anion. In fact, the oxidation potential of Bu_4NOAc is lower than that of **1** (Figure 2C, orange line).

A decrease in the oxidation current can be considered as a decrease in the diffusion coefficient of the hydrogen bond complex; thus, we attempted to reproduce the CV pattern by compu-

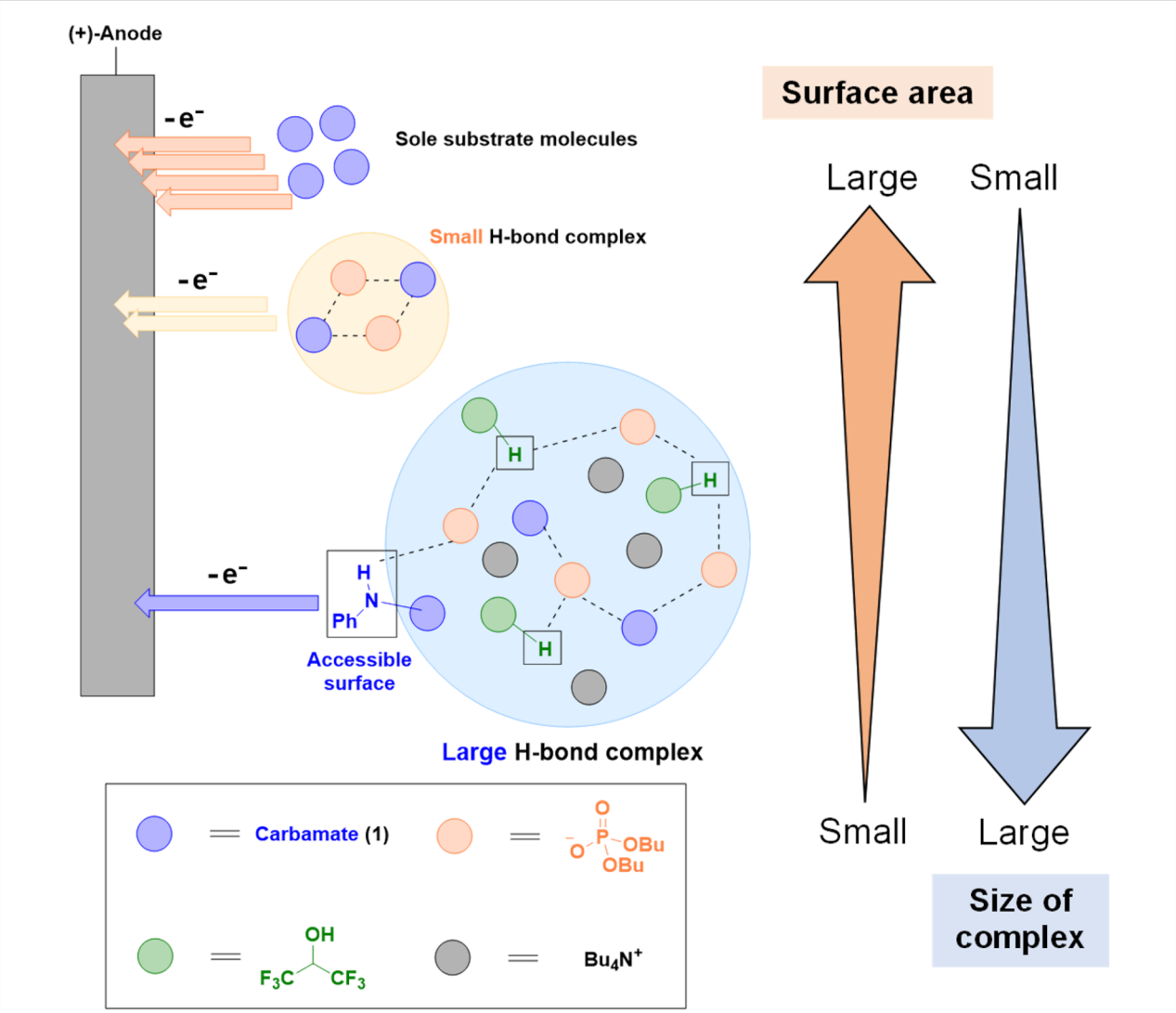

Figure 3: Plausible models illustrating the size effect of the hydrogen bond complex on the interaction efficiency with electrode surfaces.

tational simulation (Figures S1 and S2 in Supporting Information File 1) [16]. The results indicated that an excessively small diffusion coefficient (1/10- or 1/100-fold) is required to reproduce a CV pattern similar to that observed experimentally. Because the reported diffusion coefficient is only twice as small as that of the sole amide molecule [14], this simulated value is unrealistic, and we assumed that the diffusion coefficient did not affect the oxidation current.

In cathodic events, the reduction of CH_2Cl_2 primally occurred under standard conditions because the reduction wave of the blank solution appeared at approximately −1.0 V (Figure 2D, blue line). The resulting cathodically generated chloride ion (Cl^-) has a lower oxidation potential than **1** (Figure 2C, grey line); thus, it was subsequently oxidized on the anode to afford the halonium ion (Cl^+), which can react with **1** to form unstable N−Cl species (**B**) in situ (Figure 4). Although we cannot detect the chlorinated intermediate of **1**, electrolysis of *N*-propylcarbamate derivative under standard conditions gave the corresponding N−Cl species (**C**) as an unstable compound. We considered that this result as direct evidence for the plausibility of the existence of N−Cl species which driving the minor reaction pathway.

Further single-electron reduction affords the amidyl radical [17], which can react with MVK. Because *N*-alkylation also proceeded in the absence of a phosphate base but in a low yield (Table 1, entry 2), it can be concluded that only the N−Cl species contributed to *N*-alkylation in this case.

Based on the experimental and simulation results, we propose a plausible mechanism for the inter- and intramolecular hydroam-

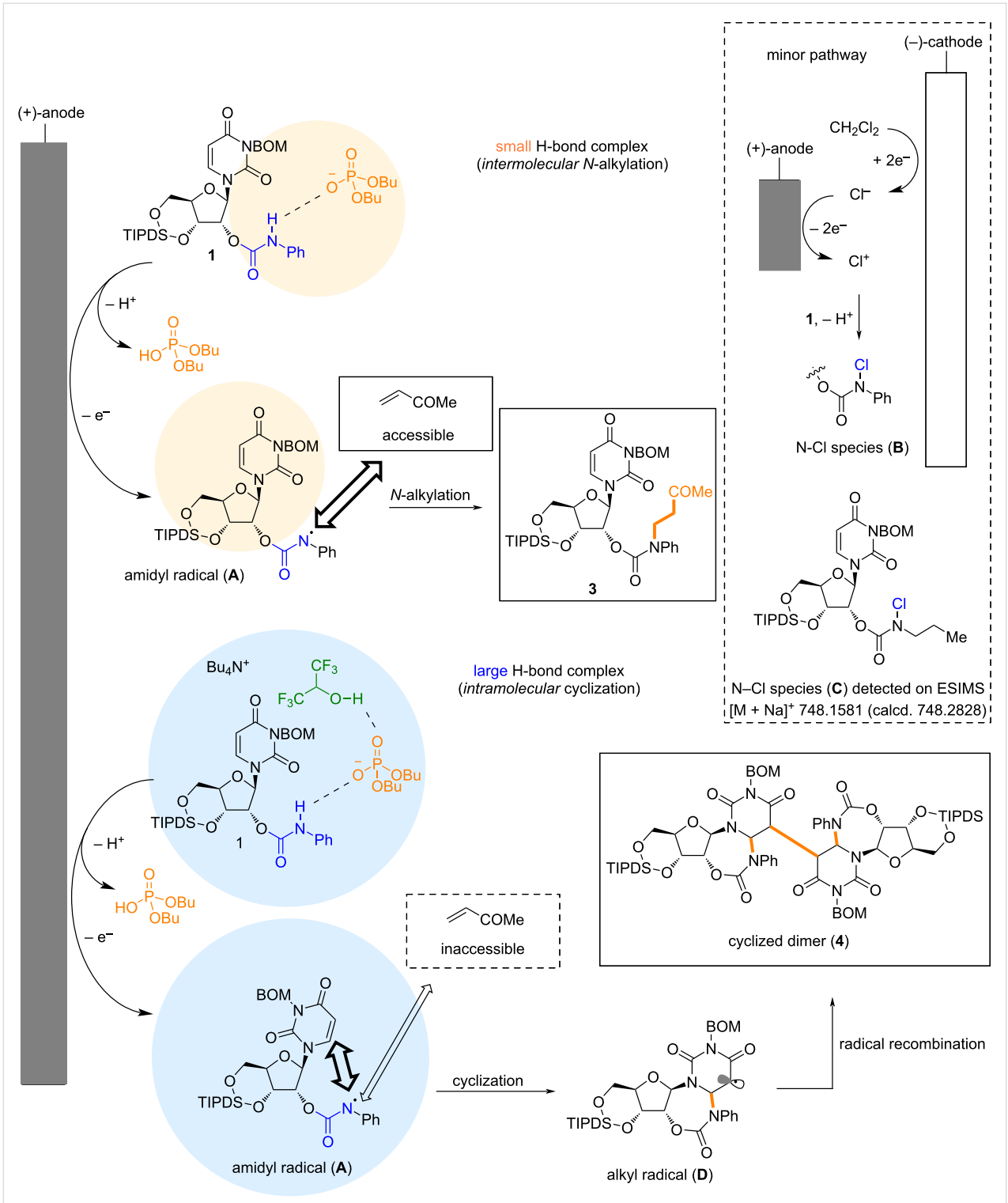

Figure 4: Plausible mechanism for the inter-/intramolecular hydroamination of **1**.

ination of **1** (Figure 4). In the *N*-alkylation reaction, anodic oxidation of a small hydrogen-bonded complex produces amidyl radical **A**. The hydrophobic MVK molecule was excluded from the highly polar environment of this complex, but the resulting amidyl radical could access MVK because it still had a large surface area for interaction with the solution interface. As mentioned above, the amidyl radical can also be generated through N–Cl species **B**.

However, the large hydrogen-bond complex, which included HFIP, prevented amidyl radical access to MVK. In this case, intramolecular radical trapping by the uracil nucleobase was preferred, leading to the formation of the cyclized alkyl radical **D**. Continuous radical recombination furnished dimer **4**.

Conclusion

We observed additive-controlled inter- and intramolecular chemoselectivity in the hydroamination of **1**. Detailed CV analysis indicated that the size of the hydrogen bond complex determined the selectivity, and HFIP played a crucial role in expanding the hydrogen bond network. These results provide fundamental insights beneficial for the design of PCET-based redox reaction systems under electrochemical conditions.

Experimental

General procedure of anodic oxidation

Compound **1** (145 mg, 0.2 mmol), Bu_4NPF_6 (387 mg, 1 mmol), CH_2Cl_2 (10 mL), phosphate base (90 mg, 0.2 mmol) and methyl vinyl ketone (32.7 μL, 0.4 mmol) were added to a test tube, which was then subjected to a constant electrical current of 5 mA (3 F/mol, 57.9 C) through the CF anode (1 × 1 cm) and the Pt cathode (1 × 1 cm). The reaction mixture was concentrated in vacuo and Et_2O (20 mL) was added. The resulting precipitate was removed by filtration through a short silica gel pad under reduced pressure. The filtrate was concentrated in vacuo and the resulting residue was subjected to ^1H NMR spectroscopy or column chromatography. A divided-cell experiment was performed using an H-type cell (4G glass filter). Compound **1** (0.2 mmol), Bu_4NPF_6 (387 mg, 1 mmol), phosphate base (90 mg, 0.2 mmol), CH_2Cl_2 (10 mL), and methyl vinyl ketone (32.7 μL, 0.4 mmol) were added to the anode chamber, and CH_2Cl_2 (10 mL), and Bu_4NPF_6 (387 mg, 1 mmol) were added to the cathode chamber. The anolyte was transferred to a round-bottomed flask, and the solvent was removed in vacuo. Et_2O (20 mL) was added to the crude mixture, and the resulting precipitate was removed by filtration through a short silica gel pad under reduced pressure. The filtrate was concentrated in vacuo and the resulting residue was subjected to ^1H NMR spectroscopy or column chromatography.

Supporting Information

Supporting Information File 1

Detailed experimental procedures, CV simulation, copies of NMR spectra.
[https://www.beilstein-journals.org/bjoc/content/supplementary/1860-5397-20-27-S1.pdf]

Funding

This work was supported by JSPS KAKENHI (Grant Nos. 22K18915 and 21H05215 to M.A. and 22H02118 23K17370, and 23H04916 to N.S.), a Grant-in-Aid for JSPS Fellows (Grant No. 22J00431 to K.O.), and JST CREST (Grant No. 18070940 to M.A.).

Author Contributions

Kazuhiro Okamoto: conceptualization; investigation; writing – original draft. Naoki Shida: conceptualization; project administration; writing – review & editing. Mahito Atobe: project administration; supervision; writing – review & editing.

ORCID® iDs

Kazuhiro Okamoto - https://orcid.org/0000-0002-3865-0362
Naoki Shida - https://orcid.org/0000-0003-0586-1216
Mahito Atobe - https://orcid.org/0000-0002-3173-3608

Data Availability Statement

All data that supports the findings of this study is available in the published article and/or the supporting information to this article.

References

1. Murray, P. R. D.; Cox, J. H.; Chiappini, N. D.; Roos, C. B.; McLoughlin, E. A.; Hejna, B. G.; Nguyen, S. T.; Ripberger, H. H.; Ganley, J. M.; Tsui, E.; Shin, N. Y.; Koronkiewicz, B.; Qiu, G.; Knowles, R. R. *Chem. Rev.* **2022,** *122,* 2017–2291. doi:10.1021/acs.chemrev.1c00374
2. Xiong, P.; Xu, H.-C. *Acc. Chem. Res.* **2019,** *52,* 3339–3350. doi:10.1021/acs.accounts.9b00472
3. Fazekas, T. J.; Alty, J. W.; Neidhart, E. K.; Miller, A. S.; Leibfarth, F. A.; Alexanian, E. J. *Science* **2022,** *375,* 545–550. doi:10.1126/science.abh4308
4. Wang, F.; Stahl, S. S. *Angew. Chem., Int. Ed.* **2019,** *58,* 6385–6390. doi:10.1002/anie.201813960
5. Zhu, Q.; Graff, D. E.; Knowles, R. R. *J. Am. Chem. Soc.* **2018,** *140,* 741–747. doi:10.1021/jacs.7b11144
6. Davies, J.; Svejstrup, T. D.; Fernandez Reina, D.; Sheikh, N. S.; Leonori, D. *J. Am. Chem. Soc.* **2016,** *138,* 8092–8095. doi:10.1021/jacs.6b04920
7. Choi, G. J.; Zhu, Q.; Miller, D. C.; Gu, C. J.; Knowles, R. R. *Nature* **2016,** *539,* 268–271. doi:10.1038/nature19811
8. Xu, F.; Zhu, L.; Zhu, S.; Yan, X.; Xu, H.-C. *Chem. – Eur. J.* **2014,** *20,* 12740–12744. doi:10.1002/chem.201404078
9. Hu, X.; Zhang, G.; Bu, F.; Nie, L.; Lei, A. *ACS Catal.* **2018,** *8,* 9370–9375. doi:10.1021/acscatal.8b02847
10. Gimisis, T.; Chatgilialoglu, C. *J. Org. Chem.* **1996,** *61,* 1908–1909. doi:10.1021/jo952218n
11. Gentry, E. C.; Knowles, R. R. *Acc. Chem. Res.* **2016,** *49,* 1546–1556. doi:10.1021/acs.accounts.6b00272
12. Kumler, W. D.; Eiler, J. J. *J. Am. Chem. Soc.* **1943,** *65,* 2355–2361. doi:10.1021/ja01252a028
13. Darcy, J. W.; Koronkiewicz, B.; Parada, G. A.; Mayer, J. M. *Acc. Chem. Res.* **2018,** *51,* 2391–2399. doi:10.1021/acs.accounts.8b00319

14. Berg, N.; Bergwinkl, S.; Nuernberger, P.; Horinek, D.; Gschwind, R. M. *J. Am. Chem. Soc.* **2021,** *143,* 724–735. doi:10.1021/jacs.0c08673
15. Dyatkin, B. L.; Mochalina, E. P.; Knunyants, I. L. *Tetrahedron* **1965,** *21,* 2991–2995. doi:10.1016/s0040-4020(01)96918-2
16. Izumiya, R.; Atobe, M.; Shida, N. *Electrochemistry* **2023,** *91,* 112003. doi:10.5796/electrochemistry.23-67010
17. Kim, H.; Kim, T.; Lee, D. G.; Roh, S. W.; Lee, C. *Chem. Commun.* **2014,** *50,* 9273–9276. doi:10.1039/c4cc03905j

License and Terms